Letter of Intent
for an experiment at 50-GeV PS

Measurement of the cross section of the Λp scattering

R. Honda, S. Kajikawa, T. Kitaoka, M. Kaneta, K. Miwa, T. Sakao, H. Tamura, S. Wada

Department of Physics, Tohoku University, Sendai, Miyagi 980-8578, Japan

H. Noumi, K. Shirotori, N. Tomida

Research Center of Nuclear Physics (RCNP), Osaka University, Ibaraki, Osaka 567-0047, Japan

T. Ishikawa

Research Center of Electron Photon Science (ELPH), Tohoku University, Sendai, Miyagi 982-0826, Japan

T. Hashimoto, Y. Ichikawa, K. Tanida

Advanced Scinence Research Center (ASRC), Japan Atomic Energy Agency (JAEA), Tokai, Ibaraki 319-1195, Japan

T. Sawada

Department of Physics, Osaka City University, Osaka 558-8585, Japan

W.-C. Chang

Institute of Physics, Academia Sinica, Taipei 11529, Taiwan

T. Yamaga

RIKEN Nishina Center, RIKEN, Wako, Saitama 351-0198, Japan

J.K. Ahn

Department of Physics, Korea University, Seoul 02841, Korea

Abstract

A high statistics Λp scattering experiment is introduced for studying P- and higher partial waves in the ΛN interaction precisely. This experiment aims to measure both the total and differential cross sections of the Λp elastic scatterings with 100 times higher statistics than those of the past experiments. The experiment will be performed at the high momentum beam line at the hadron experimental facility in the Japan Proton Accelerator Research Complex (J-PARC) using the secondary π^- beam. The $\pi^- p \to K^*(892)^0\Lambda$ reaction is chosen as the Λ production method instead of the ordinary $\pi^- p \to K^0\Lambda$ reaction in order to achieve background-free Λ tagging. As Λ is the lightest hyperon, the Λ missing-mass peak is separated from background in principle by only calculating the $p(\pi^-, K^+\pi^-)X$ missing mass without requiring the invariant mass of $K^*(892)^0$. The 350 million Λ are expected to be tagged during the 30-day beam time owing to large acceptance of the forward spectrometer, which will be constructed for the J-PARC E50 experiment, at the high-momentum beam line. The Λp scattering events are identified using the Cylindrical Detector System (CDS) currently located at the K1.8BR beam line. Finally, we expect that a few tens of thousands of the Λp scattering events are obtained for each 0.1-GeV/c momentum region of Λs ranging from 0.4 to 1.4 GeV/c.

1 Introduction

1.1 Two-body ΛN interaction

The two-body baryon-baryon (B_8B_8) interaction is the basic knowledge to explain many body systems, that is, nuclei. For understanding the properties of nuclei such as level energies and structure from the view point of the quark picture, establishment of the generalized B_8B_8 interaction including the hyperon-nucleon (YN) and the hyperon-hyperon (YY) interactions is essential. However, the lack of YN scattering data is a long standing challenge for the hypernuclear physics. To study the two-body interaction, a scattering experiment is the most straightforward way, and nucleon-nucleon scattering experiments have been extensively performed. On the other hand, both the number of YN scattering experiments and the statistical accuracy are limited due to the difficulty of the YN scattering experiment. Figure 1 shows the summary of the experimental data for the total cross sections of the Λp elastic scatterings. The horizontal axis is the Λ momentum in the laboratory system. Data points are taken from Ref. [1, 2, 3, 4, 5, 6, 7, 8]. Almost all the data points in Fig.1 are from the past bubble chamber experiments. However, the open circle data points are recent one, which was reported by the CLAS collaboration in 2019 [8]. The new Λp scattering data will be published in the near future for the fisrt time in 40 years. The number of the scattering events for each data point were a few hundreds events except for the CLAS data, and thus error bars of each data point were large. Therefore, the YN interaction have been studied by the hypernuclear data. The Λ particle is then the most well studied among the hyperons through Λ hypernuclei. ${}^{3}_{\Lambda}$H and ${}^{5}_{\Lambda}$He are good benchmark for determining the strength of the ${}^1S_0$ and ${}^3S_1$ Λp partial waves even for the recent theoretical studies [9, 10]. The ground-state spin doublet of ${}^{7}_{\Lambda}$Li also gives strong constraint to the spin dependence of the ΛN S-wave

interactions [11, 12]. As discussed in Ref. [3], determining of the scattering lengths of the ${}^1S_0$ and ${}^3S_1$ Λp partial waves was performed using only the scattering data, but the error bars were large due to limited statistics. Thus, there is almost no room to change the S-wave interactions drastically because the B_8B_8 interaction models have to reproduce the scattering data and the hypernuclear data simultaneously.

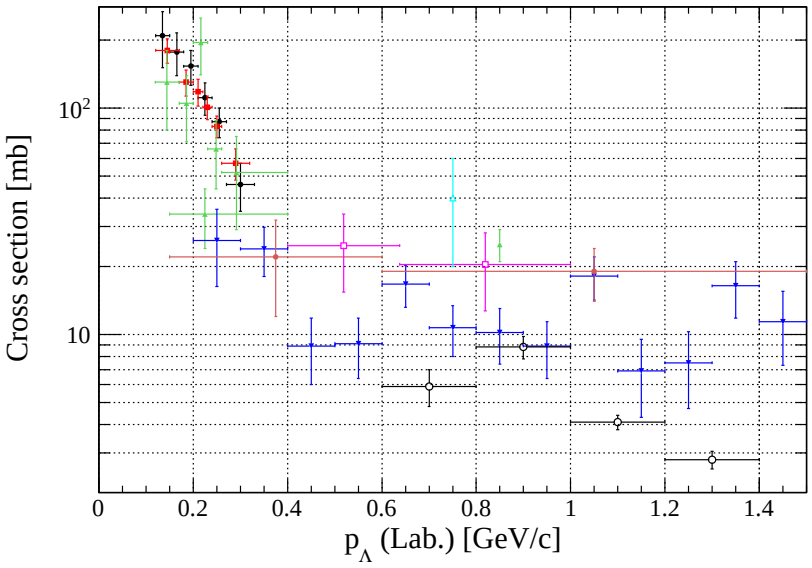

Figure 1: Total cross sections of the Λp elastic scatterings as the function of the Λ momentum in the lab. system. Data taken from Ref. [1, 2, 3, 4, 5, 6, 7, 8].

On the other hand, P- and higher partial waves in the Λp interaction have large ambiguity. From the view point of hypernuclei, there are two reasons why it is difficult to study P- and higher partial waves in the Λp interaction. One is that the binding energies of light hypernuclei are insensitive to P- and higher partial waves in the interaction [9]. The other is that the contribution from P-wave is indistinguishable from the many body effect in middle heavy hypernuclei as described later [13]. Figure 2 shows the differential cross section of the Λp elastic scatterings at $p_\Lambda = 500$ and 633 MeV/c calculated by several theoretical models. This figure is taken from Ref. [10]. The calculated results by the chiral effective field theory (bands) show that the contribution from S-waves are dominant at $p_\Lambda = 500$ MeV/c, while the sizable angular dependence is seen at $p_\Lambda = 633$ MeV/c corresponding to the $\Sigma^+ n$ threshold. However, the Jülich 04 potential (dashed) already shows the angular dependence indicating the P-wave contribution at $p_\Lambda = 500$ [14]. On the other hand, the strong angular dependence of the Nijmegen soft core 97f (dotted) is caused by the large ${}^3D_1$ contribution [15]. Note that these interaction models are well agree with the existing scattering data within the error bars. These variation is, of course, caused by the lack of the differential cross section data around these momentum regions. In order to study these partial waves, precise Λp scattering data for the Λ momentum over 400 MeV/c are essential. Both the total and differential cross

sections are necessary for the partial wave analysis.

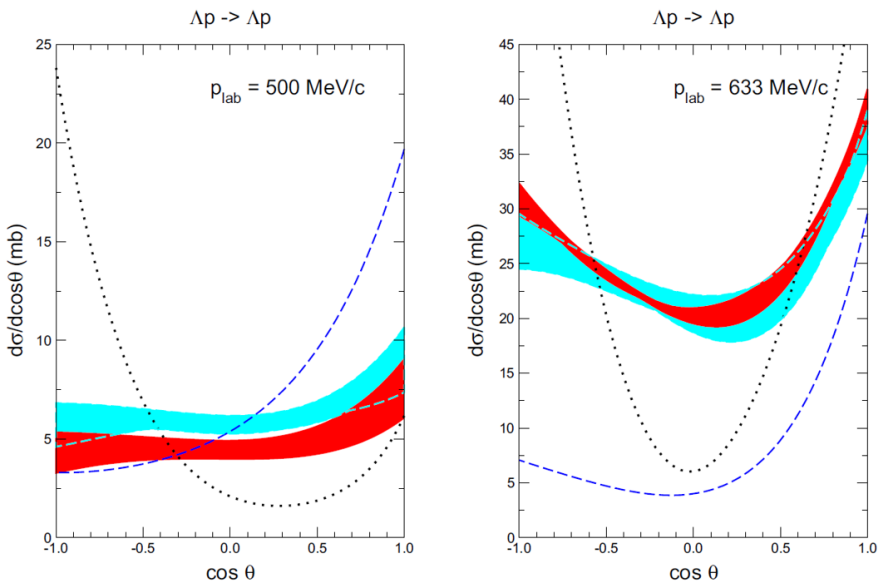

Figure 2: Calculated differential cross sections of the Λp elastic scatterings at the Λ momentum of 500 MeV/c (left) and 633 MeV/c (right), respectively. The red and blue bands show the results from the chiral effective field theory. The dashed and dotted lines are the calculated results by the Jülich 04 potential [14] and the Nijmegen soft core 97f [15], respectively. Taken from Ref. [10].

1.2 Hyperon puzzle of the neutron star

Variation of the Λp interaction models is also related to the hyperon puzzle of the neutron star. Since the Fermi energy is large enough to produce hyperons in the core of the neutron star, Λ may appear in the neutron start at 2-3 times of the normal nuclear density [16]. The maximum allowed neutron star mass is limited up to 1.3-1.4 times of the solar mass ($M_\odot$) [17] due to decreasing of neutron degeneracy pressure by the hyperon mixing. However, the quite massive neutron stars with $2M_\odot$ were observed [18][19], which cannot be explained by present knowledge of the hypernuclear physics. An additional source giving extra repulsion in order to support such the massive neutron star is necessary, and unknown many-body forces such as ΛNN, ΛNNN, etc at the higher density is a candidate. It is expected that the many-body forces in the YN sector are extracted by comparing hypernuclear binding energies measured precisely and calculated binding energies with/withtout the many-body effect. The high intensity high resolution (HIHR) beam line planed to be constructed in the J-PARC hadron experimental facility will play an important role for this porupose. However, Isaka *et al.* suggested that the present Λp interaction models are not enough precise to discuss the many-body forces from the hypernuclear data [13]. The authors calculated the hypernuclear

binding energies from $A = 9$ up to $A = 51$ based on the HyperAMD calculation using several Nijmegen extended-soft core models. These two-body models having the small difference in the P-wave intreactions provide the different binding energies for middle heavy hypernuclei. In this situation, it is difficult to extract the many-body forces, and thus improvement of the two-body interaction models are essential for the future hypernuclear study.

1.3 YN scattering experiment at J-PARC

The difficulty of YN scattering experiments is mainly due to the short life time of hyperons. As hyperons decay before reaching the detector, the past experiments adopted a hydrogen bobble chamber in order take a piture of an event topology. Accumulation of many scattering events was then technically difficult. The J-PARC E40 experiment introduced a new technique for the YN scattering experiment based on the counter experimental method and made the YN scattering experiment using the charged meson induced reaction feasible at J-PARC [22]. Here, we introduce an idea of a new experiment for the Λp scattering using the same experimental method. However, we adopt the completely different instruments in order to obtain 10 times larger statistics than that of J-PARC E40. In this experiment, we aim to update the Λp cross section data for the momentum range between from 0.4 to 1.4 GeV/c with 100 times higher statistics than those of the past bubble chamber experiments.

1.4 K^-pp production via the Λp scattering

One of the features of this experiment is the wide Λ beam momentum range up to 2 GeV/c as described in Sec. 3. This feature additionally provides an opportunity to study the K^-pp bound state. Today, it was established that the $\bar{K}N$ interaction in the isospin $I = 0$ channel is strongly attractive through the theoretical analysis of the energy shift and the width of a kaonic-hydrogen X-ray [23, 24, 25]. Akaishi and Yamazaki predicted the existence of $\bar{K}$-meson nuclear bound states [26, 27]. The simplest system among them, $\bar{K}NN$ denoted as K^-pp, was predicted as the system having the isospin $I = 1/2$ and the spin-parity $J^P = 0^-$. Following the first experimental result reported from the FINUDA collaboration [28], several experimental results were reported so far [29, 30, 31]. In J-PARC, two different experiments, that is, J-PARC E27 and E15, also reported possible candidates [32, 33], respectively. However, the values of the binding energy and the width reported by these experiments vary. For instance, the binding energies of observed candidates in E27 and E15 were $95^{+18}_{-17}(\text{stat.})^{+30}_{-20}(\text{syst.})$ MeV and $47 \pm 3(\text{stat.})^{+4}_{-6}(\text{syst.})$ MeV, respectively.

This experiment may give a conclusion by searching the peak structure of K^-pp in the plot of the total cross sections of the Λp scattering. In some experiments, the K^-pp bound state was studied by the Λp invariant mass spectrum. The observed broad width of the Λp channel suggests that the K^-pp state is strongly coupled with the Λp channel. For the Λp scattering, the K^-pp state contributes as the intermediate state. Therefore, the K^-pp bound state should be observed via the Λp scattering. The threshold $\sqrt{s}$ of the K^-pp bound system is 2.37 GeV/c^2 and corresponds to the Λ momentum of 1.5 GeV/c for the Λp scattering. By searching $\sqrt{s}$ giving the maximum total cross section, the binding energy of K^-pp is obtained. In addition, as the K^-pp bound state is considered to be produced as the P-wave

resonance for the Λp scattering, the angular distribution of the Λp scattering may support to determine the spin-parity of $K^- pp$.

2 Experimental design

2.1 Λ production and tag

Background-free Λ tagging is the key issue for the Λp scattering experiment using charged meson beams for Λ production. A neutral meson is produced via the meson induced reaction, e.g., $\pi^- p \to K^0 \Lambda$, because no neutron target at rest exists. Severe background contributed from three- and four-body decays of exited nucleons is expected and will cause heavy load to an event-filter process in a data acquisition (DAQ) system, which is described later. $s\bar{s}$ production should be tagged by finding a scattered K^+. Therefore, we newly introduce an experimental technique for the Λp scattering using the $\pi^- p \to K^*(892)^0 \Lambda$ reaction instead of $\pi^- p \to K^0 \Lambda$. $K^+ \pi^-$ decayed from $K^*(892)^0$ are detected by a magnetic spectrometer, and Λ production is identified by the missing mass technique. As described later, Λ is identified without background in the missing mass spectrum using this technique.

The other important point of Λ production is a momentum range of produced Λ. Note that we define produced Λ as the Λ beam in this experiment for brevity. The Λ beam momenta should cover the momentum range between from 0.4 GeV/c to 1.2 GeV/c or more in order to study P- and D-waves in the ΛN interaction. In principle, the maximum momentum of the Λ beam produced via $\pi^- p \to K^*(892)^0 \Lambda$ is increased as the induced π^- beam momentum is increased. In order to obtain the enough Λ yield for the expected momentum range, the π^- beam momentum more than 4 or 5 GeV/c is necessary. However, the momentum distribution of the Λ beam is broadly spread by increasing the π^- beam momentum. The yield for each momentum point is then decreased. Therefore, the high intensity π^- beam and a magnetic spectrometer having large acceptance are necessary to compensate decreasing of the yields. The high-momentum beam line of the J-PARC hadron experimental facility and the magnetic spectrometer complex proposed by the J-PARC E50 experiment [20] are suitable instruments for our purpose. Thus, we plan to perform the Λp scattering experiment at the high-momentum beam line.

2.2 Experimental setup

This experiment shares the experimental instruments with the J-PARC E50 experiment except for the detectors surrounding the liquid hydrogen (LH_2) target. Figure 3 shows the planed experimental setup. The secondary π^- beams with the momentum of 8.5 GeV/c bombard the liquid hydrogen target, of which the size are 100 mm ϕ and 570 mm in length. This target is also the same as E50 one. The reason to choose the beam momentum of 8.5 GeV/c is described in Sec. 3. The beam intensity will be 60 M/spill, which is the maximum acceptable rate for the beam detectors. Momenta of decay $K^+ \pi^-$ from $K^*(892)^0$ are measured by the forward spectrometer, of which the configuration is completely the same as the E50 setup. The forward spectrometer consists of a scintillating fiber tracker, drift chambers, timing counters (TOF wall and MRPC), and PID counters (aerogel Cherenkov counters and

a ring imaging Cherenkov counter). The forward spectrometer has large acceptance resulting in the high $K^*(892)^0$ reconstruction efficiency about 60%. The momentum resolutions of the spectrometer systems are also important for this experiment because we need to separate Σ^0 from Λ by the missing mass. When the cross section of the Λp scattering is calculated, $\rho \times L_\Lambda$ is adopted instead of the mass thickness of the LH_2 target, where ρ and L_Λ are a volume density of liquid hydrogen and a total path length of the Λ beams inside the target, respectively. As the Λ beams are produced and decayed inside the target, the total path length is necessary to obtain the number of scattering centers the Λ beams see. Thus, background-free Λ tagging is important to obtain the total path length correctly. As Λ is the lightest hyperon, Λ is free from the background caused by other hyperon production in principle. Therefore, it is not necessary to identify $K^*(892)^0$ in the $K^+\pi^-$ invariant mass spectrum. The possible background source is Σ^0 because its mass is close to the Λ mass. Figure 4 shows the expected missing mass spectrum of Λ and Σ^0 when assuming that the momentum resolution, dp/p, of the beam and the forward spectrometers are 1×10^{-3} and 2×10^{-3}, respectively. These values are the expected resolutions in E50 [20]. It is found that Λ is clearly separated from Σ^0. Thus, background-free Λ tagging is able to be achieved by these systems.

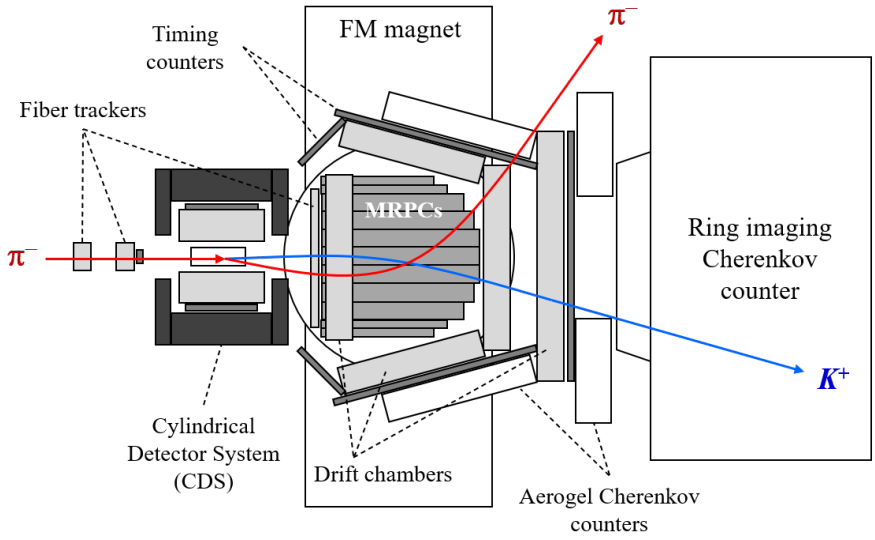

Figure 3: Schematic view of the expected experimental setup. The colored allows represent the beam π^- and decay $K^+\pi^-$ from $K^*(892)^0$. The cylindrical detector system is the surrounding detectors currently located at the K1.8BR beam line.

We will additionally install the Cylindrical Detector System (CDS), which is currently located at the K1.8BR beam line [21], as the Λp scattering detector. This system is comprised of a Cylindrical Drift Chamber (CDC), a Cylindrical Detector Hodoscope (CDH), and a solenoid magnet. CDS measures momenta of a scattered proton or decay $p\pi^-$ from a scattered Λ by the Λp scattering. The reconstruction of the scattered Λ is essential to measure the differential cross section for the forward scattering because the scattered proton when Λ is

scattered to a forward angle is slow and is stopped before reaching the detectors. CDS has the sufficient performance for the Λ reconstruction and is then suitable for this experiment. In order to install CDS, all the beam detectors and the target are moved 60 cm upstream. In addition, the target is placed 20 cm upstream from the center of CDS to optimize acceptance of CDS and the forward spectrometer.

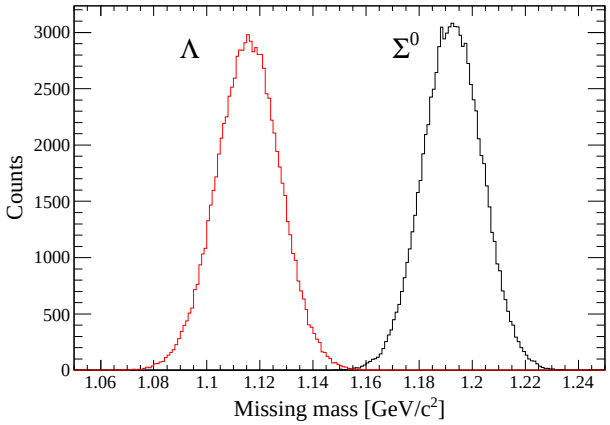

Figure 4: Expected missing mass spectrum for Λ and Σ^0.

2.3 Identification of the Λp scattering

This experiment is the double scattering experiment inside the LH_2 target, i.e., Λ is produced and is scattered again in the same target. The Λp scattering is identified by comparing the measured momentum vectors of proton or Λ with scattering kinematics. This experimental technique is based on the technique introduced by the J-PARC E40, the Σp scattering experiment [22]. The event topology inside the target is shown in Fig. 5. A Λ particle is produced via the $\pi^- p \to K^*(892)^0\Lambda$ reaction. $K^*(892)^0$ decays immediately to $K^+\pi^-$, which are measured by the forward spectrometer. Produced Λ is identified by the missing mass technique, and its missing momentum vector corresponding to the Λ beam momentum is also obtained. The angle between the Λ momentum vector and the π^- beam axis is defined as the production angle, θ_{pro}. The momentum vectors of scattered particles by the Λp scattering are obtained by measuring the scattered proton or decay products of Λ by CDS. Figure 5 shows the case where decay products of Λ are detected. Here, we can calculate the momentum of the scattered particles from the scattering angle, $\theta_{\Lambda p}$, by assuming the Λp scattering kinematics. If the measured momentum matches calculated one, that event is recognized as the Λp scattering.

2.4 Modification of CDS

As the hole size of the end guard of the CDS solenoid magnet is not enough large, the end guard causes the non-negligible acceptance loss of the forward spectrometer. The reconstruc-

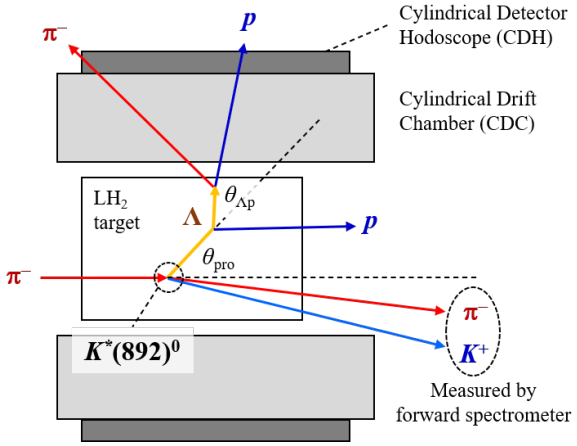

Figure 5: Event topology inside the target. The $\pi^- p \to K^*(892)^0\Lambda$ reaction followed by the Λp scattering is shown. θ_{pro} and $\theta_{\Lambda p}$ are the production angle of Λ and the Λp scattering angle, respectively.

tion efficiency of $K^*(892)^0$ is recovered from 41% to 62% by widening the hole diameter from 30 cm to 40 cm. Details of the reconstruction efficiency is described in Sec. 3.

2.5 Data acquisition system

The high-momentum beam line plans to employ the streaming DAQ system, which is based on data streaming of all the data without any trigger and event filtering in personal computers. In the event-filter processes, the event is selected according to not only simple timing coincidence but also the momentum analysis based on tracking. Finally, the rough mass spectroscopy is performed. As background events will be strongly suppressed in the DAQ system, the DAQ (trigger) rates can be reduced a few kHz even with the π^- beam of 60 M/spill. On the other hand, tagging of $s\bar{s}$ production before the tracking process is essential to reduce unnecessary tracking that is just CPU load. Therefore, the $\pi^- p \to K^*(892)^0\Lambda$ reaction is reasonable from the view point of the DAQ system because K^+ in the final state guarantees $s\bar{s}$ production.

3 Simulation

3.1 Λ yield estimation

The past experimental data of the total cross section of $\pi^- p \to K^*(892)^0\Lambda$ exist only for beam momentum up to 6 GeV/c [34, 35, 36]. Unfortunately, there is no data around the beam momentum of 8 GeV/c, but the theoretical analysis of the past data predicts the cross section more than 6 GeV/c [37]. Figure 6 shows the past data and the theoretical calculation of the total cross sections of $\pi^- p \to K^*(892)^0\Lambda$ [37] as the function of s/s_{th}, where s_{th} is the threshold s of $K^*(892)^0 + \Lambda$. Although the momentum dependence of the theoretical

predictions are different, the smaller one is adopted considering it conservatively in this estimation. Thus, the production cross section of Λ at 8.5 GeV/c corresponding to $s/s_{th} = 4.2$ is assumed to be 20 μb. The differential cross section taken from Ref. [36] is shown in

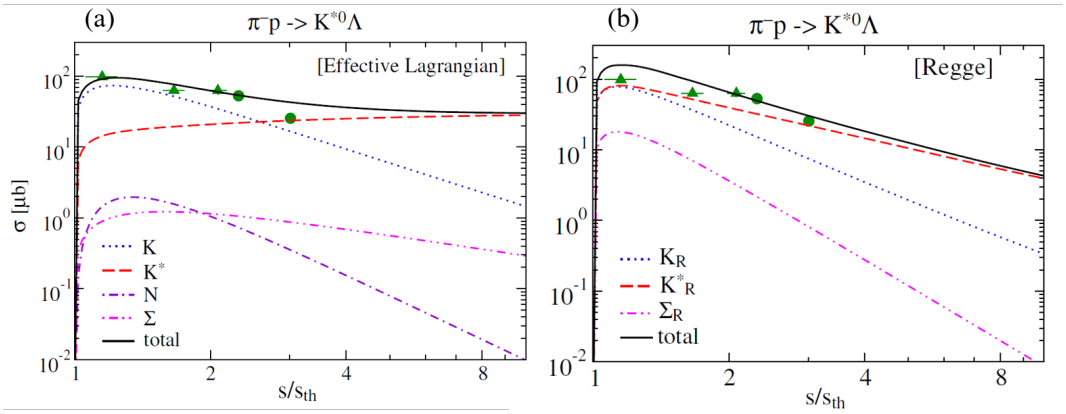

Figure 6: Calculated total cross sections of $\pi^- p \to K^*(892)^0\Lambda$ together with the past experimental data. (a) Calculated result using the effective Lagrangian. (b) Calculated rust using the Regge model. Taken from Ref. [37].

Fig. 7. The data is fitted by a 6th order polynomial as represented by the blue curve and is used in the Monte Carlo simulation. As mentioned in Ref. [37], the contribution from the t-channel is dominant. It results in the meson forward peak in the differential cross section.

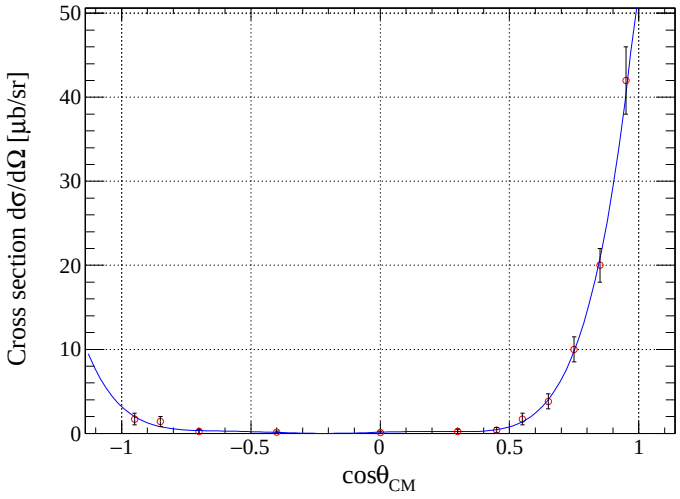

Figure 7: Differential cross section of $\pi^- p \to K^*(892)^0\Lambda$ at 6 GeV/c. Data points are taken from Ref. [36]. The blue curve represents the fitting result by a 6th order polynomial.

The experimental setup shown in Fig. 3 is reproduced in the Monte Carlo simulation based on the Geant4 simulator. In this simulation, Λ and $K^*(892)^0$ are generated according to the differential cross section shown in Fig. 7. The black histograms in Fig. 8 show the momentum distribution and the production angle distribution of Λ, respectively, when $K^*(892)^0$ decays to $K^+\pi^-$. Those histograms represent the distributions of the detectable events in this reaction. The red (hatched) histograms are those for the reconstructed events by the forward spectrometer. The reconstruction efficiency between 0.3 to 2.0 GeV/c is 62%. The momentum dependence of the reconstruction efficiency is also shown in Fig.9. Figure 8 (b) shows the important property, that is, the produced Λ has the large production angle owing to the high beam momentum. As CDS does not have acceptance for the angle of less than about 50 degrees, the forward Λp scattering cannot be detected if the production angle is small. Owing to this property, the experiment has the sensitivity for the forward scattering as described later.

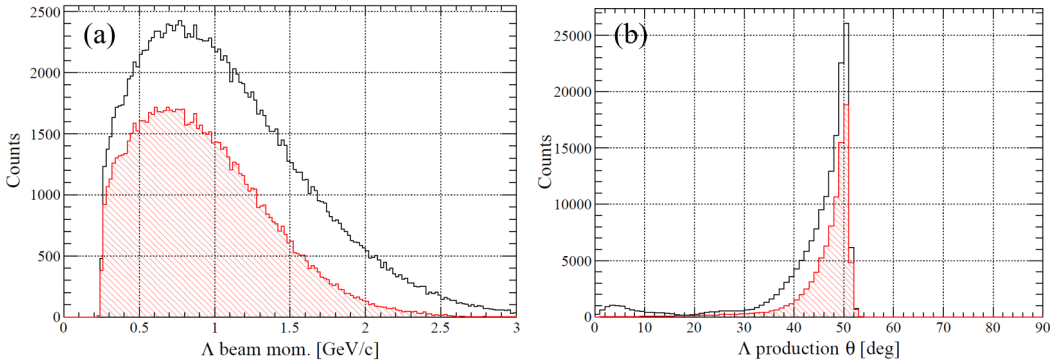

Figure 8: (a) Momentum distribution of produced Λ. (a) Production angle distribution of Λ.

Here, we estimate the yield of the Λ beam during the 30-day beam time. By assuming the total cross section of 20 μb and the beam intensity of 60 M/spill, 2900 Λ particles are produced via the $\pi^- p \to K^*(892)^0\Lambda$ reaction per spill. As the branching ratio of the $K^*(892)^0 \to K^+\pi^-$ mode is 66%, 1900 Λ/spill are detectable. If we assume that the DAQ efficiency and the analysis efficiency are 0.95 and 0.7, respectively, 830 Λ particles are tagged in one spill. Note that the acceptance of the forward spectrometer is taken into account. By considering the accelerator efficiency of 0.9, the number of tagged Λ in 30-day is 350 million Λ in total. This is roughly 15 times larger statistics than that of the Σ^- beam obtained in the J-PARC E40 experiment. The yields in each momentum region are plotted in Fig. 10.

3.2 Yield estimation of Λp scattering

The Λp scattering is also generated following the $\pi^- p \to K^*(892)^0\Lambda$ reaction in the simulation. We assumed that the total cross section is 20 mb and its angular distribution is isotropic. First, we estimated the detection efficiencies of CDS for the scattered proton or decay products of Λ after scattering. The definition of the detection is that the particle reaches to CDH. The angular distribution of the CDS detection efficiencies is shown in Fig. 11 at

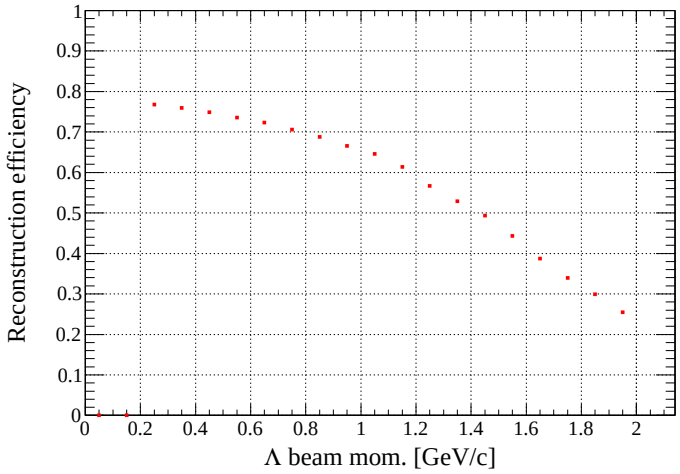

Figure 9: Momentum dependence of the $K^*(892)^0$ reconstruction efficiency.

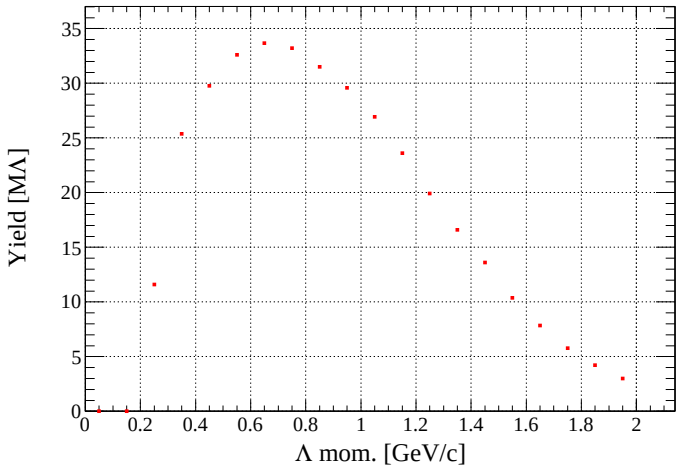

Figure 10: Expected Λ beam yields in 30-day beam time as the function of the Λ beam momentum.

the momentum range of $0.6 < p_\Lambda < 0.8$ GeV/c. The horizontal axis is the $cos\theta_{\rm CM}$ of the Λp scattering, where $cos\theta_{\rm CM} = 1$ corresponds to forward scattering of Λ. The efficiency for proton is about 0.6, but it suddenly drops around $cos\theta_{\rm CM} = 0.6$ because the proton energy is insufficient to reach CDH. On the other hand, the efficiency for Λ is not zero even in the forward angle. As only the $\Lambda \to p\pi^-$ decay mode is detectable, the detection efficiency for Λ already includes the branching ratio of 0.64.

Finally, we estimated the yields of the Λp scattering events. If the total cross section of the Λp scattering is 20 mb, about 3900 scatterings are occurred per 1 million Λ beams. The

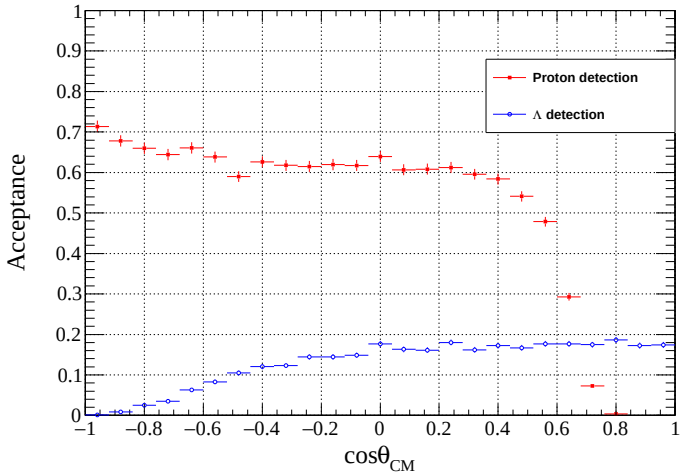

Figure 11: Angular distribution of the CDS detection efficiencies for the scattered proton and the Λ after scattering. Red (closed square) points and blue (open circle) points represent those for proton and Λ, respectively. The horizontal axis is $cos\theta_{\rm CM}$ of the Λp scattering.

number of the Λp scattering events expected in 30-day beam time is calculated by considering the CDC tracking efficiency of 0.9 and the CDS detection efficiencies shown in Fig. 11. The results are plotted in Fig. 12. Note that analysis cuts, e.g., vertex selection, background rejection etc, are not taken into account in this estimation. However, if the yields are halved, we are able to plot at least 10 new data points from 0.4 to 1.4 GeV/c.

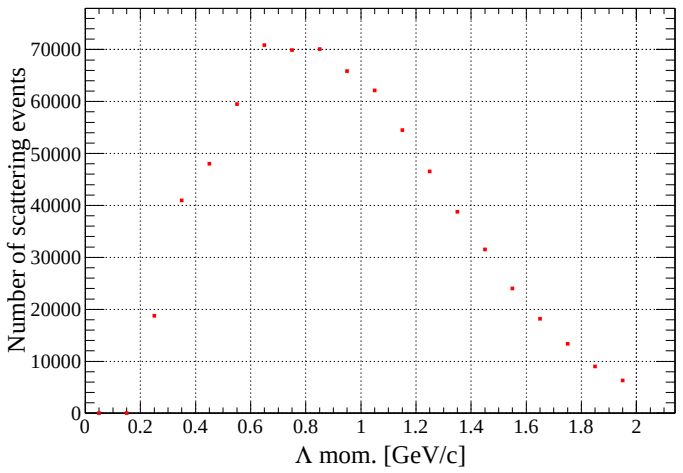

Figure 12: Expected yields of the Λp scattering as the function of the Λ beam momentum.

4 Summary

Partial waves except for S-wave in the ΛN interaction models still have large ambiguity due to the lack of the Λp scattering data. For understanding not only hypernuclei but also inside of the neutron star, improvement of the two-body ΛN interaction models are desired. In order to overcome this situation, we introduce an experiment for the Λp elastic scattering. This experiment aims to update both the total and differential cross sections for the Λ beam momentum between from 0.4 to 1.4 GeV/c with 100 times higher statistics than those of the past bubble chamber experiments. In addition, the Λ beam momentum range up to 2 GeV/c allows us to study the K^-pp bound state. The peak search for the total cross section plot of the Λp elastic scattering provides biding energy information. The angular distribution around the peak position may support to determine the spin-parity of K^-pp.

The experiment will be performed at the high momentum beam line in the hadron experimental facility in J-PARC. The 60 M/spill π^- beams with the momentum of 8.5 GeV/c are bombarded to the liquid hydrogen target. We select the $\pi^- p \to K^*(892)^0\Lambda$ reaction instead of $\pi^- p \to K^0\Lambda$ in order to avoid background contamination from non-strangeness reactions. Λ is tagged by the missing mass technique by measuring the decay products of $K^*(892)^0$ by the forward spectrometer for the J-PARC E50 experiment [20]. Owing to large acceptance of the forward spectrometer, 350 million Λ will be tagged during the 30-day beam time. CDS in the K1.8BR beam line [21] will be installed around the hydrogen target to detect the Λp scatterings. The detection efficiencies of CDS for the scattered proton or Λ are 0.6 and 0.2, respectively, By detecting the scattered Λ, CDS is able to cover all the $cos\theta$ region. Finally, we expect to obtain a few tens of thousands of the Λp scattering events for each momentum region every 100 MeV/c. This is 100 times higher statistics than those of the past bubble chamber experiments.

References

[1] B. Sechi-Zorn, B. Kehoe, and R.A. Burnstein, Phys Rev 175, 1735 (1968).

[2] B. Sechi-Zorn, R. A. Burnstein, T. B. Day, B. Kehoe, and G.A. Snow, Phys Rev Lett. 13, 282 (1964).

[3] G. Alexander, U. Karshon, A. Shapira *et al.,* Phys Rev. 173, 1452 (1968).

[4] J.A. Kadyk, G. Alexander, J.H. Chan, P. Gaposchkin, G.H. Trilling, Nucl. Phys. B27, 13 (1971).

[5] Thomas H. Groves, Phys Rev. 129, 1372 (1963).

[6] G. Alexander, J.A. Anderson, F.S. Crawford, Jr., W. Laskar, and L.J. Lloyd, Phys. Rev. Lett. 7, 348 (1961).

[7] F.S. Crawford, Jr., M. Cresti, M.L. Good, F.T. Solmitz, M.L. Stevenson, and H.K. Ticho, Phys. Rev. Lett. 2, 174 (1959).

[8] J. Rowley, K. Hicks, and John Price, Talk in 52nd Reimei workshop. https://asrc.jaea.go.jp/soshiki/gr/hadron/workshop/reimei2019

[9] H. Le, J. Haidenbauer, U.-G. Meißner, A. Nogga, Phys. Lett. B 801, 135189 (2020).

[10] J. Haidenbauer, U.-G. Meißner, A. Nogga, Eur. Phys. J. A, 56 (2020).

[11] D.J. Millener, Nucl. Phys. A 639, 135c (2001).

[12] D.J. Millener, Nucl. Phys. A 754, 48c (2005).

[13] M. Isaka, Y. Yamamoto, and Th. A. Rijken, Phys. Rev. C **95**, 044308 (2017).

[14] J. Haidenbauer and U.-G. Meißner, Phys. Rev. C 72, 044005 (2005).

[15] T.A. Rijken, V.G.J. Stocks, Y. Yamamoto, Phys. Rev. C 59, 21 (1999).

[16] R. Knorren, M. Prakash, and P. J. Ellis, Phys. Rev. C **52-6**, 3470 (1995).

[17] Z. H. Li and H.-J. Schulze, Phys. Rev. C **78**, 028801 (2008).

[18] P. B. Demorest *et al.,* Nature **467**, 1081-1083 (2010).

[19] J. Antoniadis et al., Science **340**, 1233232 (2013)

[20] H. Noumi *et al.,* Proporsal for an experiment at J-PARC, 'Charmed Baryon Spectroscopy via the (π, D^{*-}) reaction', http://j-parc.jp/researcher/Hadron/en/pac_1301/pdf/P50_2012-19.pdf

[21] K. Agari, S. Ajimura, G. Beer *et al.,* Prog. Theor. Exp. Phys. 02B011 (2012).

[22] K. Miwa *et al.,* Proporsal for an experiment at J-PARC, 'Measurement of the cross section of Σp scattering', http://j-parc.jp/researcher/Hadron/en/pac_1101/pdf/KEK_J-PARC-PAC2010-12.pdf

[23] M. Iwasaki *et al.,* Phys. Rev. Lett. 78, 3067 (1997).

[24] G. Beer *et al.,* Phys. Rev. Lett. 94, 212302 (2005).

[25] M. Bazzi *et al.,* Phys. Lett. B 704, 113 (2011).

[26] Y. Akaishi and T. Yamazaki, Phys. Rev. C 65, 044005 (2002).

[27] T. Yamazaki and Y. Akaishi, Phys. Lett. B 535, 70 (2002).

[28] M. Agnello *et al.,* Phys. Rev. Lett. 94, 212303 (2005).

[29] T. Yamazaki *et al.,* Phys, Rev. Lett. 104, 132502 (2010).

[30] G. Agakishiev *et al.,* Phys. Lett. B 742, 242 (2015).

[31] O .Vazquez Doce *et al.,* Phys, Lett. B 758, 134 (2016).

[32] Y. Ichikawa *et al.,* Prog. Theor. Exp. Phys. 021D01 (2015).

[33] S. Ajimura, H. Asano, G. Beer *et al.,* Phys. Lett. B 789, 620 (2019).

[34] Orin I. Dahl *et al.,* Phys. Rev. 163-5, 1337 (1967).

[35] M. Aguilar-Benitez *et al.,* Z. Physik C, Particles and Fields 6, 195-215 (1980).

[36] David J. Crennell *et al.,* Phys. Rev. D 6-5, 1220 (1972).

[37] Sang-Ho Kim *et al.,* Phys. Rev. D 92, 094021 (2015).